ELSEVIER

Journal of Hazardous Materials B138 (2006) 46–52

Journal of Hazardous Materials

www.elsevier.com/locate/jhazmat

# Reaction paths and efficiency of photocatalysis on $TiO_2$ and of $H_2O_2$ photolysis in the degradation of 2-chlorophenol

Marco Bertelli, Elena Selli *

*Dipartimento di Chimica Fisica ed Elettrochimica, Università degli Studi di Milano, Via Golgi 19, I-20133 Milano, Italy*

Received 10 March 2006; received in revised form 10 May 2006; accepted 10 May 2006
Available online 20 May 2006

**Abstract**

The kinetics of 2-chlorophenol (2-CP) degradation and mineralization in the aqueous phase was investigated under irradiation at 254 nm, employing either photocatalysis in the presence of titanium dioxide, or hydrogen peroxide photolysis, to compare the efficiency of these photoinduced advanced oxidation techniques. Photocatalysis under 315–400 nm wavelength irradiation was also investigated. The concentration versus time profiles of the degradation intermediates catechol, chloro- and hydroxy-hydroquinone allowed the identification of the reaction paths prevailing under the different experimental conditions. Efficient C–Cl bond cleavage occurred as a consequence of direct light absorption by 2-CP, while hydroxyl radicals, photogenerated at the water–photocatalyst interface or during $H_2O_2$ photolysis, were the main oxidation agents, able to attack both 2-CP and its degradation intermediates. Highest degradation and mineralization efficiencies were achieved under $H_2O_2$ photolysis at 254 nm.
© 2006 Elsevier B.V. All rights reserved.

*Keywords:* 2-Chlorophenol degradation; UV irradiation; Photocatalysis; Titanium dioxide; Hydrogen peroxide photolysis

## 1. Introduction

Chlorophenols represent an important class of very common water pollutants. Because of their extensive use as fungicides, herbicides and wood preservatives [1], they can easily be found in soils and in aquatic environments. Other sources include the waste incineration or disinfection of sewage and industrial wastewater with chlorine, as well as discharges from paper mills, releasing them as by-products of chlorine-based bleaching [2]. Chlorophenols are persistent water pollutants under environmental conditions, due to the stability of the C–Cl bond, which is also responsible for their toxicity [3]. Most of them have been listed as toxic or priority pollutants by both the US Environmental Protection Agency and the European Commission [4,5].

The increasing awareness of the possible environmental effects of chlorophenols has led to the demand for limiting their use and for the development of new methods of treating contaminated waters. Their degradation by conventional techniques is rather challenging, because of their stability and high solubility in water. Particular emphasis has been given in recent years to the use of advanced oxidation processes (AOPs) for water purification, some of which are based on either direct or sensitized photolysis; the degradation of chlorophenols by these means has been recently reviewed [6]. AOPs present the great advantage that they completely remove organic contaminants from the environment, not only from the aqueous phase, by transforming them into other organic compounds and finally into innocuous inorganic species. A correct application of AOPs requires the identification and possibly the monitoring of all intermediate species, which might be more toxic and/or persistent than the original contaminants.

In the present work detailed kinetic studies are reported on the aqueous phase degradation of 2-chlorophenol (2-CP), chosen as model chlorinated aromatic pollutant, employing two photoinduced AOPs, namely photocatalysis in the presence of titanium dioxide and hydrogen peroxide photolysis. 2-CP degradation under both photocatalysis [7–13] and $H_2O_2$ photolysis [14–18] has already been investigated by different research groups. Aim of the present study is a comparison between the water depollution efficiency of the two techniques employing the same irradiation source, also in relation to the rate of overall mineralization and to the intermediate species produced during 2-CP degradation. The concentration profiles of the aromatic intermediates have thus been monitored during the photodegradation

* Corresponding author. Tel.: +39 02 5031 4237; fax: +39 02 5031 4300.
*E-mail address:* elena.selli@unimi.it (E. Selli).

0304-3894/$ – see front matter © 2006 Elsevier B.V. All rights reserved.
doi:10.1016/j.jhazmat.2006.05.030

treatments, aiming at identifying the reaction paths prevailing in each case and at ascertaining their effectiveness, also in relation to the evolution of the overall toxicity.

## 2. Experimental

### 2.1. Materials

2-Chlorophenol and the identified degradation intermediates catechol (CT), chloro-hydroquinone (CH), hydroxy-hydroquinone (HQ), hydroquinone and chloro-benzoquinone were all analytical grade reagents, purchased from Aldrich. Hydrogen peroxide (30 wt.%) was also an Aldrich product. Degussa P25 titanium dioxide (mainly anatase) was employed as photocatalyst. Water purified by a Milli-Q water system (Millipore) was used in the preparation of solutions and suspensions.

### 2.2. Apparatus

Most degradation runs were carried out in the already described 800-mL magnetically stirred reactor [19], employing a quartz jacketed 15 W immersion low pressure mercury arc lamp (Jelosil, model NSL15) as irradiation source. This lamp emitted exclusively at 253.7 nm, with a radiation flow of $2.8 \times 10^{-6}$ einstein $s^{-1}$, according to ferrioxalate actinometry [20]. The reactor was thermostated at $(30 \pm 1)\,^{\circ}C$ by continuous water recirculation through an external glass jacket.

Some photocatalytic runs were performed at the same temperature in a cylindrical Pyrex 400-mL vessel [21]. In this case the light source was an external Jelosil, model HG 200, 250 W iron halogenide lamp, emitting in the 315–400 nm wavelength range, with a radiation flow on the reactor equal to $2.0 \times 10^{-5}$ einstein $s^{-1}$ [20].

### 2.3. Procedure

In order to avoid any undesired loss of 2-CP during the runs, the two reactors were almost completely filled with aqueous solutions or suspensions containing an initial 2-CP concentration around $1.0 \times 10^{-3}$ M. Titanium dioxide (up to 0.5 g $L^{-1}$) was added directly in the reactors. Pre-equilibration of 2-CP in $TiO_2$ suspensions for more than 30 min did not induce any difference in the 2-CP photodegradation behavior. The initial concentration of hydrogen peroxide was up to $1.8 \times 10^{-2}$ M. All runs were carried out in duplicate, under atmospheric conditions, and lasted 6 h. The lamps were always switched on at least 30 min before filling the reactors, which were maintained tightly closed and magnetically stirred during the runs.

Samples (2 mL) were withdrawn at different reaction times by means of a syringe, through a silicon rubber septum of the reactors. Prior to analysis, $TiO_2$ was separated from the suspensions by centrifugation at 4800 rpm for 60 min. 2-CP and its degradation by-products were determined by gas chromatography (GC) employing an Agilent 6890 apparatus with FID detection and a HP-5 (5%-phenyl)-methylpolysiloxane capillary column, with helium as carrier gas, flowing at 3.5 mL $min^{-1}$. One microliter of the solution (or supernatant) was injected in the apparatus, followed by a temperature ramp from 80 up to 270 °C at 10 °C $min^{-1}$. The extent of mineralization was determined through total organic carbon (TOC) analysis using a Shimadzu TOC-5000A analyzer in the non-purgeable organic carbon mode. The absorption spectra of the aqueous phase were also recorded during some runs, employing a Perkin-Elmer Lambda 16 apparatus. An Amel 334-B instrument was used for pH measurement on withdrawn samples.

Table 1
First order rate constants of 2-chlorophenol degradation, initial and final pH values, percent degradation and mineralization attained after 6 h irradiation at 254 nm in the presence of different amounts of $TiO_2$

| $TiO_2$ (g $L^{-1}$) | $10^5 \times k$ ($s^{-1}$) | 2-CP removal (%) | Mineralization (%) | $pH_i$ | $pH_f$ |
|---|---|---|---|---|---|
| – | 12.2 ± 0.2 | 92 | 21 | 6.5 | 3.0 |
| 0.1 | 6.8 ± 0.3 | 75 | 31 | 6.6 | 3.2 |
| 0.3 | 5.3 ± 0.3 | 67 | 35 | 6.6 | 3.4 |
| 0.5 | 4.45 ± 0.14 | 60 | 38 | 6.6 | 3.5 |

The amount of 2-CP adsorbed on $TiO_2$ at equilibrium was measured in suspensions containing 0.1 g $L^{-1}$ of $TiO_2$ and up to $5 \times 10^{-3}$ M of each aromatic compound. After 24 h-long stirring in the dark at 30 °C, the suspensions were centrifuged and the residual 2-CP concentration in the supernatant was determined by spectrophotometric analysis.

## 3. Results and discussion

### 3.1. Direct photolysis

2-CP confirmed to be reasonably photostable in aqueous solution under irradiation in the 315–400 nm wavelength range [22], while it underwent fast photolysis under irradiation at 254 nm, though the photon flow was almost 10-fold lower in this case (see Section 2.2). 2-CP concentration decreased according to a first order rate law, up to more than 90% transformation after 6 h. The rate constant measured under these conditions is reported in Table 1. The pH of the solution decreased during the run from an initial value of 6.5 down to ca. 3. The mineralization extent, monitored by total organic carbon analysis, was only around 20% after 6 h, indicating the extensive formation of organic by-products. Catechol was identified by GC analysis as the main aromatic intermediate under these conditions, as already reported [8,11,12]. Lower concentrations of other by-products, most probably cyclopentadiene carboxylic acids [23,24] and a low (ca. $10^{-5}$ M), almost constant concentration of phenol were also evidenced. This confirms that an efficient cleavage of the C–Cl bond occurs from the electronically excited state of 2-CP produced by direct light absorption at 254 nm.

### 3.2. Photocatalytic degradation in the presence of $TiO_2$

2-CP photocatalytic degradation was investigated under irradiation at 254 nm in the presence of different amounts of titanium dioxide particles (UV + $TiO_2$). The 2-CP concentration profiles (Fig. 1) reasonably fit an apparent first order rate law, as in

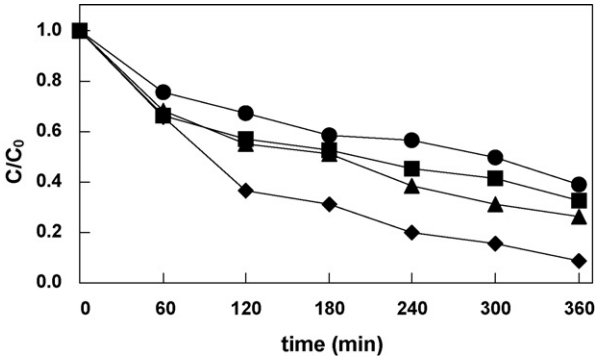


Fig. 1. Residual 2-CP concentration under irradiation at 254 nm (diamonds) and under photocatalysis at 254 nm (UV + $TiO_2$) in the presence of 0.1 g $L^{-1}$ (triangles), 0.3 g $L^{-1}$ (squares) and 0.5 g $L^{-1}$ (circles) of $TiO_2$.

previous studies [8,10,13]. The calculated rate constants are reported in Table 1, together with the percent 2-CP degradation and mineralization attained after 6 h and with the initial and final pH values of the irradiated suspensions. 2-CP photodegradation under 254 nm irradiation clearly proceeded faster in the absence of $TiO_2$ particles and became progressively slower in the presence of progressively higher $TiO_2$ amounts. This may appear surprising at first sight. However, a similar behavior has been reported under irradiation either at 254 nm [12] or containing low wavelength components [10], while in general a rate increase was observed upon photocatalyst addition under irradiation at longer wavelengths [8,12].

Of course, concomitant direct 2-CP photolysis and photocatalysis on $TiO_2$ occur under irradiation at 254 nm. The fact that, with increasing the fraction of light absorbed (and scattered) by the semiconductor particles, 2-CP underwent progressively slower degradation, indicates that the photocatalytic degradation path was slower than direct 2-CP photolysis. Moreover, the progressively lower pH decrease observed in the presence of higher amounts of $TiO_2$ (Table 1) can be related to a lower amount of acids released as a consequence of the C–Cl bond cleavage. This is confirmed by the concentration profiles of the intermediate species, discussed in Section 3.4.

By contrast, photocatalytic conditions ensured faster mineralization. As shown in Table 1, progressively higher percent mineralization was attained after 6 h irradiation in the presence of progressively higher amounts of photocatalyst: by-products are relatively more reactive under photocatalysis than under simple photolysis, not all of them being able to absorb light at 254 nm and undergo direct photolysis.

A first order decrease of the substrate concentration under photocatalysis is in agreement with the well-established Langmuir–Hinshelwood model [25], under conditions of low substrate adsorption on the photocatalyst. 2-CP adsorption measurements evidenced that an almost constant, low percent amount of 2-CP (around 4%) was adsorbed at equilibrium on 0.1 g $L^{-1}$ of $TiO_2$ from aqueous suspensions containing up to $1 \times 10^{-3}$ M 2-CP. Indeed, the amount of 2-CP adsorbed on $TiO_2$, $n_{ads}$, was found to linearly increase with increasing 2-CP molar concentration $C$ (M) in the aqueous phase, according to the following equation: $n_{ads}$ (mol $g^{-1}$) = $(0.44 \pm 0.03) \times C$ (M). Thus, adsorption was far from saturation at an overall 2-CP concentration of $1.0 \times 10^{-3}$ M, in agreement with the pseudo-first order rate law observed for its photocatalytic degradation.

Photocatalysis on semiconductors is known to produce •OH radicals in water, through the interface oxidation of hydroxide anions or water molecules adsorbed on the semiconductor surface by the holes photogenerated in the semiconductor valence band [26]. The so produced •OH radicals initiate the degradation of aromatic compounds by direct attack to the aromatic rings. The photogenerated valence band holes may also induce the direct oxidation of molecules adsorbed on the semiconductor, leading to radical cations, which subsequently interact with oxygen-containing species. These two photocatalytic reaction paths, frequently yielding the same products [26], can hardly be distinguished in most cases.

Under irradiation at 254 nm, direct 2-CP photolysis appears to be faster than any photocatalytic degradation path. Aiming at isolating the effects of photocatalysis at the water–oxide interface from 2-CP photolysis in the aqueous phase, 2-CP degradation was investigated also under irradiation in the 315–400 nm wavelength range in the presence of 0.1 g $L^{-1}$ of $TiO_2$. 2-CP concentration was found to decrease under such conditions, with an apparent first order rate constant equal to $(6.9 \pm 0.4) \times 10^{-5}$ $s^{-1}$, which is almost identical to that obtained in the presence of 0.1 g $L^{-1}$ of $TiO_2$ under irradiation at 254 nm (Table 1). A direct comparison of the photon efficiencies in the two irradiation systems is quite difficult. Indeed, the photon flow emitted by the low pressure lamp was lower than that of the iron halogenide lamp, but all the 254 nm photons were able to excite the semiconductor, while only a fraction of those emitted in the 315–400 nm range was sufficiently energetic to achieve this. However, a lower pH decrease (i.e. from 6.5 to ca. 5.0) was observed under longer wavelengths irradiation, which is compatible with a lower rate of 2-CP dechlorination. Thus, 2-CP dechlorination would mainly be consequent to direct absorption of light by 2-CP, occurring only under irradiation at wavelengths below 300 nm.

### 3.3. Photoinduced degradation in the presence of $H_2O_2$

Aiming at having a deeper insight into the effective reactivity of •OH radicals and at avoiding the detrimental light scattering effect due to the presence of semiconductor particles, 2-CP photoinduced degradation was investigated in aqueous solutions initially containing different amounts of hydrogen peroxide (UV + $H_2O_2$). $H_2O_2$ absorbs light at 254 nm and undergoes O–O bond cleavage from its electronically excited state, leading to hydroxyl radicals production, with almost unitary quantum yield [27].

2-CP degradation and mineralization were found to be very fast under UV + $H_2O_2$ conditions. In particular, as shown in Fig. 2, almost complete 2-CP degradation was achieved in 30 min with the highest initial $H_2O_2$ concentration employed in the present work ($1.8 \times 10^{-2}$ M). The rate of 2-CP photodegradation in the presence of $H_2O_2$ was higher than under direct photolysis and it increased for higher initial $H_2O_2$ contents (Fig. 2), in line with earlier reports [15,18]. On the basis of the molar extinction coefficients of 2-CP ($\varepsilon = 443$ $M^{-1}$ $cm^{-1}$) and

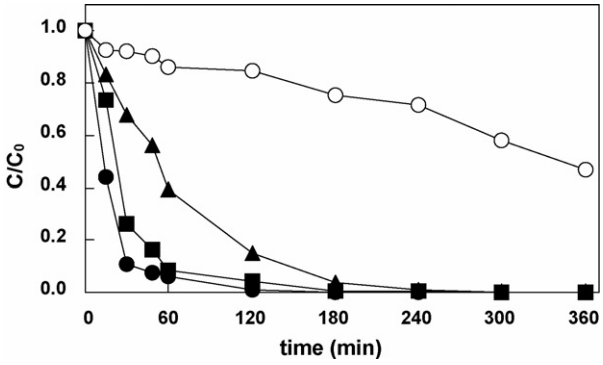


Fig. 2. Residual 2-CP concentration (full symbols) and TOC content (open symbols) under hydrogen peroxide photolysis (UV + $H_2O_2$). Initial $H_2O_2$ concentration: $4.5 \times 10^{-3}$ M (triangles), $9.0 \times 10^{-3}$ M (squares) and $1.8 \times 10^{-2}$ M (circles).

$H_2O_2$ ($\varepsilon = 18.7\ M^{-1}\ cm^{-1}$) [28] at 254 nm, the fraction of light absorbed by $1.8 \times 10^{-2}$ M $H_2O_2$ at the beginning of the runs was ca. 43%. This fraction decreased to 28 and 16% for initial $H_2O_2$ concentrations equal to $9.0 \times 10^{-3}$ and $4.5 \times 10^{-3}$ M, the rest of light being directly absorbed by 2-CP. Thus, the concentration profiles shown in Fig. 2 clearly demonstrate that •OH radicals attack on the aromatic ring in the aqueous phase is much faster than 2-CP direct photolysis or any interface process involving 2-CP at the water–semiconductor interface. The rate constant for •OH radical addition to 2-CP to produce a dihydroxy-chlorocyclohexadienyl radical has been reported to be $1.2 \times 10^{10}\ M^{-1}\ s^{-1}$ [29].

Overall mineralization once again proceeded at a lower rate with respect to 2-CP degradation, though at a higher rate with respect to UV + $TiO_2$ conditions. For instance, mineralization proceeded only up to 53% after 6 h under $1.8 \times 10^{-2}$ M hydrogen peroxide photolysis at 254 nm (Fig. 2). The initial pH of the solution ranged between 5.2 and 6.3. Progressively lower pH values, ranging between 2.8 and 2.6, were attained after 6 h irradiation in solutions initially containing increasing $H_2O_2$ concentration, indicating that •OH radical attack on the aromatic ring also results in the formation of acidic species consequent to efficient C–Cl bond scission.

### 3.4. Aromatic degradation intermediates and reaction paths

Catechol (CT) was the main aromatic intermediate under direct 2-CP photolysis at 254 nm; its concentration constantly increased during the runs, up to ca. $10^{-4}$ M after 6 h. CT was detected during 2-CP degradation under both UV + $TiO_2$ and UV + $H_2O_2$ conditions with $\lambda_{irr} = 254$ nm, but not under irradiation in the 315–400 nm range. Thus, CT does not form in high yield under photocatalysis [8], i.e. –Cl substitution by –OH groups is not expected to occur with high yield through •OH radical attack at the semiconductor–water interface. Indeed, CT concentration profiles under UV + $TiO_2$ conditions were progressively lower, the higher was the $TiO_2$ amount (Fig. 3), all of them being much lower than that detected under 254 nm irradiation in the absence of photocatalyst. Thus, under UV + $TiO_2$ conditions CT mainly formed through direct 2-CP photolysis,

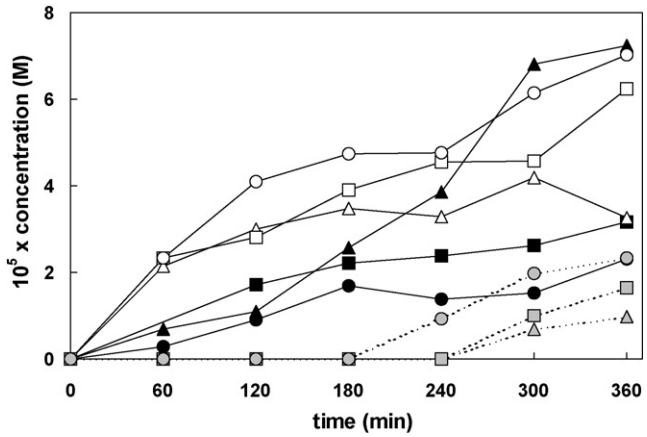


Fig. 3. Concentration profiles of CT (full symbols), CH (open symbols) and HQ (grey symbols) detected during the photocatalytic (UV + $TiO_2$) degradation of 2-CP at 254 nm in the presence of 0.1 g $L^{-1}$ (triangles), 0.3 g $L^{-1}$ (squares) and 0.5 g $L^{-1}$ (circles) of $TiO_2$.

which proceeded at a lower rate, the higher was the fraction of light absorbed (and scattered) by $TiO_2$. Moreover, progressively higher final pH values were obtained with increasing the $TiO_2$ amount within the irradiated suspension (Table 1).

CT is known to strongly adsorb on $TiO_2$ [30], forming long wavelength absorbing complexes. In the absence of paths leading to its formation in the aqueous phase, i.e. under irradiation with $\lambda_{irr} > 300$ nm, CT might be undetectable in the presence of $TiO_2$, even if it forms at the semiconductor–water interface, because it undergoes rapid photocatalytic degradation directly at the interface.

As shown in Fig. 4, CT appeared from the very beginning of the runs also under UV + $H_2O_2$ conditions, but in this case it soon reached a maximum concentration, which was higher for lower initial $H_2O_2$ concentrations, and then disappeared. In the presence of the highest $H_2O_2$ concentration ($1.8 \times 10^{-2}$ M) CT was detected in very low amount only at the beginning of the runs and completely disappeared in less than 30 min. The higher amount of •OH radicals produced by $H_2O_2$ photolysis

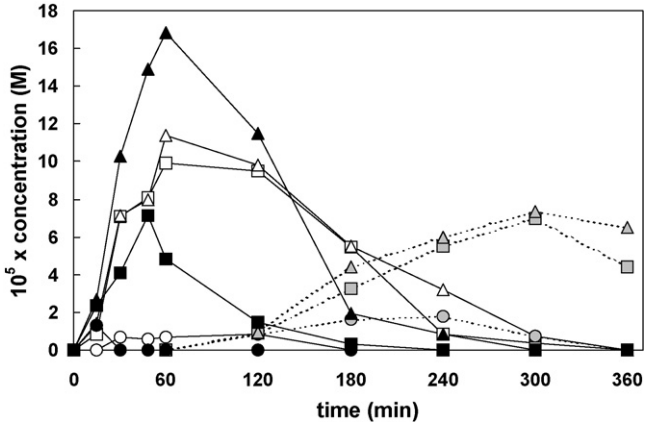


Fig. 4. Concentration profiles of CT (full symbols), CH (open symbols) and HQ (grey symbols) detected during the degradation of 2-CP under hydrogen peroxide photolysis at 254 nm (UV + $H_2O_2$). Initial $H_2O_2$ concentration: $4.5 \times 10^{-3}$ M (triangles), $9.0 \times 10^{-3}$ M (squares) and $1.8 \times 10^{-2}$ M (circles).

in the aqueous phase clearly contributes in the transformation of CT into other oxygenated by-products [31], undergoing ring opening and final mineralization (vide infra).

Chloro-hydroquinone (CH) was also identified as intermediate species under both UV + $TiO_2$ and UV + $H_2O_2$ conditions, but not in the case of 2-CP direct photolysis at 254 nm. Thus, it forms only in the presence of •OH radicals. As shown in Fig. 3, under UV + $TiO_2$ conditions its concentration at the beginning of the runs was higher than CT concentration and it attained higher levels in the presence of higher $TiO_2$ amounts, exhibiting an exactly opposite trend with respect to CT. Thus, another 2-CP degradation path, parallel to dechlorination, is at work under UV + $TiO_2$ conditions, involving •OH radicals attack onto the aromatic ring in the *para* position with respect to the –OH group of 2-CP [8,12]. Moreover, the higher was the $TiO_2$ amount, the higher was the CH concentration increase and the lower was the CT concentration profile (Fig. 3). This confirms that CT mainly forms through direct 2-CP photolysis at 254 nm, while CH results from a reaction path involving •OH radicals on the photocatalyst surface. Indeed, CH was detected in rather high concentration (ca. $2.5 \times 10^{-4}$ M) under 315–400 nm irradiation in the presence of $TiO_2$, but it rapidly disappeared, followed by the appearance of poly-hydroxylated aromatic species.

CH concentration sharply increased at the beginning of the runs under UV + $H_2O_2$ conditions up to relatively high levels (Fig. 4), especially for low initial $H_2O_2$ amounts, and then continuously declined during the rest of the run. CH did not accumulate and totally disappeared in less than 2 h, when the initial concentration of $H_2O_2$ was high.

Thus, CT and CH appear to form in parallel reaction paths under both UV + $TiO_2$ and UV + $H_2O_2$ conditions. A third major by-product appeared later on, i.e. hydroxy-hydroquinone (HQ), formed either from CH, by photoinduced C–Cl bond scission and Cl substitution with an OH group, or from CT, through further •OH radical attack on the aromatic ring. Under UV + $TiO_2$ conditions (Fig. 3) the amount of HQ was smaller than under UV + $H_2O_2$ conditions (Fig. 4). As shown in Fig. 3, HQ concentration profile stayed higher, the higher was the $TiO_2$ amount, indicating that it presumably forms mainly from CH, rather than from CT.

The different reaction paths of 2-CP photodegradation in the presence of $TiO_2$ or $H_2O_2$ are summarized in Scheme 1. The greater was the $TiO_2$ amount (absorbing and scattering light), the slower were 2-CP degradation and CT formation (prevalently occurring through direct 2-CP photolysis) and the greater was CH formation (Fig. 3), consequent to •OH radicals attack in the *para* position. Under $H_2O_2$ photolysis, both CT and CH were immediately detected at the beginning of 2-CP degradation, indicating that •OH radicals photoproduced in the aqueous phase may attack the aromatic ring either at the *ortho* position, leading to Cl substitution, or at the *para* position, leading to OH addition. Both intermediates rapidly transformed into HQ (Fig. 4) and in other more oxidized species. Further information on the reaction paths leading to overall mineralization was obtained by investigating CT and CH photodegradation.

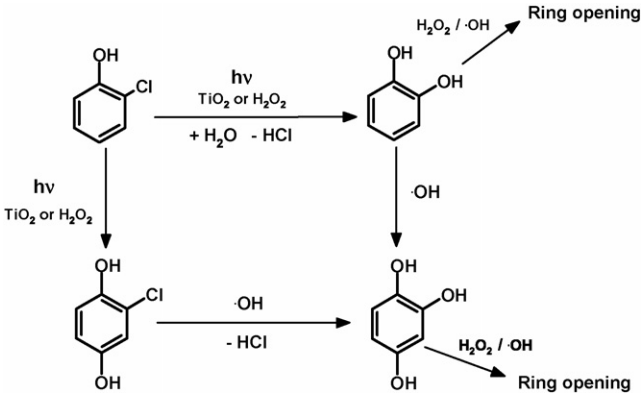


Scheme 1. Reaction paths of 2-CP degradation under photocatalysis on $TiO_2$ and $H_2O_2$ photolysis at 254 nm.

### 3.5. CT and CH degradation paths

CT (initial concentration $1.0 \times 10^{-3}$ M) was found to undergo rather slow degradation under photolysis at 254 nm, according to a first order kinetics, with a rate constant equal to $(2.42 \pm 0.05) \times 10^{-5}\ s^{-1}$, i.e. much lower than the rate constant of 2-CP degradation under photolysis (Table 1). The pH of the irradiated solution decreased from 5.3 to 3.9 after 6 h. Although 2-CP and CT exhibit very similar absorption spectra, 2-CP undergoes faster degradation under 254 nm excitation because of the photolability of the C–Cl bond. The relatively higher photostability of CT explains why 2-CP mineralization proceeds very slowly under simple photolysis (Table 1).

CT underwent faster degradation under irradiation in the presence of $TiO_2$ ($0.1\ g\ L^{-1}$), with an apparent first order rate constant of $(4.5 \pm 0.3) \times 10^{-5}\ s^{-1}$. The pH of the irradiated suspension decreased from 5.9 to 3.5. CT forms inner sphere complexes on the $TiO_2$ surface [30] and thus is expected to adsorb more strongly than 2-CP; its degradation through photocatalytic processes at the water–semiconductor interface was faster than its direct photolysis in the aqueous phase. Thus, CT accumulated in greater amount, the lower was the $TiO_2$ content of the irradiated suspensions (Fig. 3). HQ and other benzenetriol isomers were the main degradation by-product of CT degradation under UV + $TiO_2$ conditions, together with other unidentified species, compatible with the aromatic ring opening (vide infra).

The effect of $H_2O_2$ photolysis on CT could not be investigated, as CT was found to be unstable in the presence of $1.8 \times 10^{-2}$ M $H_2O_2$, rapidly undergoing oxidation of the two adjacent –OH groups, followed by ring opening [32]. Consequently, CT could hardly be detected under irradiation in solutions initially containing $1.8 \times 10^{-2}$ M $H_2O_2$ (Fig. 4).

Also CH photodegradation was investigated starting from a $1.0 \times 10^{-3}$ M initial concentration. CH underwent degradation through direct photolysis at 254 nm according to a first order rate law, with a relatively high rate constant equal to $(1.10 \pm 0.06) \times 10^{-4}\ s^{-1}$. Dechlorination was the main degradation path [33], yielding hydroquinone with ca. 80% yield after 3 h, in line with the sudden pH drop from 6.0 to 2.8. No HQ could be detected in the reaction medium.

CH photoinduced degradation was even faster under photocatalysis, proceeding with a rate constant of $(1.41 \pm 0.04) \times 10^{-4}\ s^{-1}$ in the presence of $0.1\ g\ L^{-1}$ of $TiO_2$, with a pH drop from 6.5 to 2.6. Hydroquinone and mostly HQ were detected as by-products.

Also CH was found to be unstable in the presence of $H_2O_2$ $1.8 \times 10^{-4}$ M and to transform quantitatively into chlorobenzoquinone. Such species could not be detected under 254 nm irradiation, because it absorbs light very efficiently (its molar absorption coefficient at 254 nm is $1.62 \times 10^4\ M^{-1}\ cm^{-1}$) and undergoes rapid photoconversion with high quantum yield [7]. Thus, very low CH amounts could be detected under irradiation in the presence of a high concentration of hydrogen peroxide (Fig. 4).

Finally, HQ was detected during the photocatalytic degradation of CT and during CH photolysis, both in the presence and in the absence of $TiO_2$. Efficient dechlorination is testified in this case by the observed pH decrease. HQ degradation under photocatalytic conditions implied ring opening and formation of acyclic acids [32]. Indeed, the minor peaks appearing in our GC analysis were found to be compatible with the presence of degradation products generated from muconic acid (1,3-butadiene, 1,4-dicarboxylic acid).

## 4. Conclusions

The present kinetic analysis on 2-CP degradation photoinduced in the presence of either $TiO_2$ or $H_2O_2$ leads to the following conclusions:

- Efficient aryl–Cl bond cleavage occurs under irradiation at 254 nm, with an expected reduction of toxicity.
- Hydroxyl radicals, photoproduced either at the semiconductor–water interface, or from $H_2O_2$ photolysis in the aqueous phase, efficiently oxidize 2-CP and its degradation intermediates. $^{\bullet}$OH radicals in the aqueous phase attack the aromatic ring of 2-CP either at the *ortho* position, leading to Cl substitution, or at the *para* position, leading to OH addition.
- $TiO_2$ particles have a shielding effect on 2-CP degradation and CT formation, while a greater amount of CH forms through $^{\bullet}$OH radicals attack in the *para* position.
- Hydrogen peroxide photolysis at 254 nm is most effective for achieving fast 2-CP degradation and high dechlorination and mineralization efficiencies.

## References


[1] J. Paasivirta, Organochlorine compounds in the environment, Water Sci. Technol. 20 (1988) 119–129.

[2] K.R. Krijgsheld, A. Van der Gen, Assessment of the impact of the emission of certain organochlorine compounds on the aquatic environment. Part I. Monochlorophenols and 2,4-dichlorophenols, Chemosphere 15 (1986) 825–860.

[3] H. Roques, Chemical Water Treatment, VCH, Weinheim, Germany, 1996.

[4] EPA, July 2002, http://www.scorecard.org.

[5] EC Decision 2455/2001/EC.

[6] M. Pera-Titus, V. García-Molina, M.A. Banos, J. Giménez, S. Esplugas, Degradation of chlorophenols by means of advanced oxidation processes: a general review, Appl. Catal. B: Environ. 47 (2004) 219–256.

[7] T. Sehili, P. Boule, J. Lemaire, Photocatalysed transformation of chloroaromatic derivatives on zinc oxide. III. Chlorophenols, J. Photochem. Photobiol. A: Chem. 50 (1989) 117–127.

[8] J.-C. D'Oliveira, G. Al-Sayyed, P. Pichat, Photodegradation of 2- and 3-chlorophenol in $TiO_2$ aqueous suspensions, Environ. Sci. Technol. 24 (1990) 990–996.

[9] Y. Ku, R.-M. Leu, K.-C. Lee, Decomposition of 2-chlorophenol in aqueous solution by UV irradiation with the presence of titanium dioxide, Water Res. 30 (1996) 2569–2578.

[10] R.-A. Doong, C.-H. Chen, R.A. Maithreepala, S.-M. Chang, The influence of pH and cadmium sulfide on the photocatalytic degradation of 2-chlorophenol in titanium dioxide suspensions, Water Res. 35 (2001) 2873–2880.

[11] G. Li Puma, P.L. Yue, Effect of the radiation wavelength on the rate of photocatalytic oxidation of organic pollutants, Ind. Eng. Chem. Res. 41 (2002) 5594–5600.

[12] I. Ilisz, A. Dombi, K. Mogyorósi, A. Farkas, I. Dékány, Removal of 2-chlorophenol from water by adsorption combined with $TiO_2$ photocatalysis, Appl. Catal. B: Environ. 39 (2002) 247–256.

[13] N.N. Rao, A.K. Dubey, S. Mohanty, P. Khare, R. Jain, S.N. Kaul, Photocatalytic degradation of 2-chlorophenol: a study of kinetics, intermediates and biodegradability, J. Hazard. Mater. B101 (2003) 301–314.

[14] D.W. Sundstrom, B.A. Weir, H.E. Klei, Destruction of aromatic pollutants by UV light catalyzed oxidation with hydrogen peroxide, Environ. Prog. 8 (1989) 6–11.

[15] Y.-S. Shen, Y. Ku, K.-C. Lee, The effect of light absorbance on the decomposition of chlorophenols by ultraviolet radiation and U.V./$H_2O_2$ processes, Water Res. 29 (1995) 907–914.

[16] A.K. De, B. Chaudhuri, S. Bhattacharjee, B.K. Dutta, Estimation of OH radical reaction rate constants for phenol and chlorinated phenols using UV/$H_2O_2$ photo-oxidation, J. Hazard. Mater. 64 (1999) 91–104.

[17] M. Hugül, R. Apak, S. Demirci, Modeling the kinetics of UV/hydrogen peroxide oxidation of some mono-, di-, and trichlorophenols, J. Hazard. Mater. B77 (2000) 193–208.

[18] M.A. Barakat, J.M. Tseng, C.P. Huang, Hydrogen peroxide-assisted photocatalytic oxidation of phenolic compounds, Appl. Catal. B: Environ. 59 (2005) 99–104.

[19] M. Bertelli, E. Selli, Kinetic analysis on the combined use of photocatalysis, $H_2O_2$ photolysis and sonolysis in the degradation of methyl *tert*-butyl ether, Appl. Catal. B: Environ. 52 (2004) 205–212.

[20] C.G. Hatchard, C.A. Parker, A new sensitive chemical actinometer. II. Potassium ferrioxalate as a standard chemical actinometer, Proc. R. Soc. London A 235 (1956) 518–536.

[21] M. Mrowetz, E. Selli, Effects of iron species in the photocatalytic degradation of an azo dye in $TiO_2$ aqueous suspensions, J. Photochem. Photobiol. A: Chem. 162 (2004) 89–95.

[22] V. Ragaini, E. Selli, C.L. Bianchi, C. Pirola, Sono-photocatalytic degradation of 2-chlorophenol in water: kinetic and energetic comparison with other techniques, Ultrason. Sonochem. 8 (2001) 251–258.

[23] Z. Shi, M.E. Sigman, M.M. Ghosh, R. Dabestani, Photolysis of 2-chlorophenol in surfactant solutions, Environ. Sci. Technol. 31 (1997) 3581–3587.

[24] F. Bonnichon, G. Grabner, C. Richard, B. Lavédrine, Mechanism of 2-iodophenol photolysis in aqueous solution, New J. Chem. 27 (2003) 591–596.

[25] C.S. Turchi, D.F. Ollis, Photocatalytic degradation of organic water contaminants: mechanisms involving hydroxyl radical attack, J. Catal. 122 (1990) 178–192.

[26] M.R. Hoffmann, S.T. Martin, W. Choi, D.W. Bahnemann, Environmental applications of semiconductor photocatalysis, Chem. Rev. 95 (1995) 69–96.

[27] J.H. Baxendale, J.A. Wilson, Photolysis of hydrogen peroxide at high light intensities, Trans. Faraday Soc. 53 (1957) 344–356.

[28] E. Selli, I.R. Bellobono, M.L. Raimondi, Photosynthetic membranes. 21. Immobilization of catalase by photochemically grafted ultrafiltration membranes, Angew. Makromol. Chem. 196 (1992) 169–177.

[29] N. Getoff, S. Solar, Radiolysis and pulse radiolysis of chlorinated phenols in aqueous solutions, Radiat. Phys. Chem. 28 (1986) 443–450.
[30] R. Rodríguez, M.A. Blesa, A.E. Regazzoni, Surface complexation at the $TiO_2$ (anatase)/aqueous solution interface: chemisorption of catechol, J. Colloid Interface Sci. 177 (1996) 122–131.
[31] A. Hirvonen, M. Trapido, J. Hentunen, J. Tarhanen, Formation of hydroxylated and dimeric intermediates during oxidation of chlorinated phenols in aqueous solution, Chemosphere 41 (2000) 1211–1218.
[32] X. Li, J.W. Cubbage, T.A. Tetzlaff, W.S. Jenks, Photocatalytic degradation of 4-chlorophenol. 1. The hydroquinone pathway, J. Org. Chem. 64 (1999) 8509–8524.
[33] A. Rossi, A. Tournebize, P. Boule, Phototransformation of chlorohydroquinone in aqueous solution, J. Photochem. Photobiol. A: Chem. 85 (1995) 213–216.